Geophysical Research Letters

RESEARCH LETTER
10.1029/2020GL087867

Global Heat Uptake by Inland Waters

I. Vanderkelen[1], N. P. M. van Lipzig[2], D. M. Lawrence[3], B. Droppers[4], M. Golub[5], S. N. Gosling[6], A. B. G. Janssen[4], R. Marcé[7,8], H. Müller Schmied[9,10], M. Perroud[11], D. Pierson[5], Y. Pokhrel[12], Y. Satoh[13], J. Schewe[14], S. I. Seneviratne[15], V. M. Stepanenko[16,17], Z. Tan[18], R. I. Woolway[19], and W. Thiery[1,15]

[1]Department of Hydrology and Hydraulic Engineering, Vrije Universiteit Brussel, Brussels, Belgium, [2]Department of Earth and Environmental Sciences, KU Leuven, Leuven, Belgium, [3]National Center for Atmospheric Research, Boulder, CO, USA, [4]Water Systems and Global Change Group, Wageningen University & Research, Wageningen, The Netherlands, [5]Department of Ecology and Genetics, Uppsala University, Uppsala, Sweden, [6]School of Geography, University of Nottingham, Nottingham, UK, [7]Catalan Institute for Water Research, Girona, Spain, [8]University of Girona, Girona, Spain, [9]Institute of Physical Geography, Goethe University Frankfurt, Frankfurt an Main, Germany, [10]Senckenberg Leibniz Biodiversity and Climate Research Centre (SBiK-F), Frankfurt am Main, Germany, [11]Institute for Environmental Sciences, University of Geneva, Geneva, Switzerland, [12]Department of Civil and Environmental Engineering, Michigan State University, East Lansing, MI, United States, [13]Center for Global Environmental Research, National Institute for Environmental Studies, Tsukuba, Japan, [14]Transformation Pathways, Potsdam Institute for Climate Impact Research, Potsdam, Germany, [15]Institute for Atmospheric and Climate Science, ETH Zurich, Zurich, Switzerland, [16]Research Computing Center, Moscow State University, Moscow, Russia, [17]Faculty of Geography, Moscow State University, Moscow, Russia, [18]Pacific Northwest National Laboratory, Richland, WA, USA, [19]Centre for Freshwater and Environmental Studies, Dundalk Institute of Technology, Dundalk, Ireland

Key Points:
- We use a unique combination of lake models, hydrological models, and Earth System models to quantify global heat uptake by inland waters
- Heat uptake by inland waters over the industrial period amounts up to 2.6×10^{20} J, or 3.6% of the continental heat uptake
- The thermal energy of the water trapped on land due to dam construction (26.8×10^{20} J) is 10.4 times larger than inland water heat uptake

Supporting Information:
- Supporting Information S1

Correspondence to:
I. Vanderkelen,
inne.vanderkelen@vub.be

Citation:
Vanderkelen, I., van Lipzig, N. P. M., Lawrence, D. M., Droppers, B., Golub, M., Gosling, S. N., et al. (2020). Global heat uptake by inland waters. *Geophysical Research Letters*, *47*, e2020GL087867. https://doi.org/10.1029/2020GL087867

Received 11 MAR 2020
Accepted 27 MAY 2020
Accepted article online 4 JUN 2020

©2020. The Authors.
This is an open access article under the terms of the Creative Commons Attribution License, which permits use, distribution and reproduction in any medium, provided the original work is properly cited.

Abstract Heat uptake is a key variable for understanding the Earth system response to greenhouse gas forcing. Despite the importance of this heat budget, heat uptake by inland waters has so far not been quantified. Here we use a unique combination of global-scale lake models, global hydrological models and Earth system models to quantify global heat uptake by natural lakes, reservoirs, and rivers. The total net heat uptake by inland waters amounts to $2.6 \pm 3.2 \times 10^{20}$ J over the period 1900–2020, corresponding to 3.6% of the energy stored on land. The overall uptake is dominated by natural lakes (111.7%), followed by reservoir warming (2.3%). Rivers contribute negatively (-14%) due to a decreasing water volume. The thermal energy of water stored in artificial reservoirs exceeds inland water heat uptake by a factor ~10.4. This first quantification underlines that the heat uptake by inland waters is relatively small, but non-negligible.

Plain Language Summary Human-induced emissions of CO_2 and other greenhouse gases cause energy accumulation in the Earth system. Oceans trap most of this excess energy, thereby largely buffering the warming of the atmosphere. However, the fraction of excess energy stored in lakes, reservoirs, and rivers is currently unknown, despite the high heat capacity of water. Here we quantify this human-induced heat storage, and show that it amounts up to 3.6% of the energy stored on land, while covering 2.58% of the land surface. The increase in heat storage from 1900 to 2020 is dominated by warming of lakes. The thermal heat contained in the water stored in man-made reservoirs is about ten times larger. Our study overall highlights the importance of inland waters–next to oceans, ice and land–for buffering atmospheric warming, especially on regional scale.

1. Introduction

Increasing greenhouse gas concentrations in the atmosphere cause a net heat uptake in the Earth System. Over 90% of this extra thermal energy is stored in the oceans, causing ocean warming and global sea level rise through thermal expansion (Rhein et al., 2013). The most recent estimates of heat uptake are described in the Special Report on the Ocean and Cryosphere in a Changing Climate by the Intergovernmental Panel on Climate Change. The report concludes that the ocean has taken up $4.35 \pm 0.8 \times 10^{21}$ J year^{-1} in the upper 700 m of water and $2.25 \pm 0.64 \times 10^{21}$ J year^{-1} between the depths of 700–2000 m, respectively (averages of 1998–2017 compared to 1971–1990), and attributes this increase to anthropogenic forcings

(Bindoff et al., 2019). The remaining excess heat is taken up by melting sea and land ice, by specific heating and water evaporation in the atmosphere and by warming of the continents (Trenberth, 2009).

Despite the key role of heat uptake in driving Earth system response to greenhouse gas forcing, currently little is known about global-scale heat uptake by inland waters. Inland waters include natural lakes, man-made reservoirs, rivers, and wetlands, with lakes covering 1.8% of the global land area (Messager et al., 2016) and rivers 0.58% of the global non-glaciated land area (Allen & Pavelsky, 2018). However, the abundance and total area covered by inland waters (natural and artificial) is continuously changing (Pekel et al., 2016). For example, reservoir expansion following dam construction experienced a marked acceleration during the 1960s and 1970s, now covering 0.2% of the global land area (Lehner et al., 2011). Despite occupying <3% of the global land surface, inland waters play an important role in the climate system (e.g., Choulga et al., 2019; Subin et al., 2012; Vanderkelen et al., 2018a) and are sentinels of climate change (e.g., Adrian et al., 2009; Schewe et al., 2014). Compared to other types of land surfaces, water (i) has a higher specific heat capacity, (ii) typically has a lower albedo, (iii) allows for radiation penetration below the surface, and (iv) seasonally mixes warmer surface masses to deeper layers. Consequently, inland waters are generally regarded as heat reservoirs compared to adjacent land. In addition, lake surface temperatures have been observed to have increased rapidly in recent decades, in some locations even faster than ambient air temperatures (O'Reilly et al., 2015; Schneider & Hook, 2010).

To quantify the heat uptake by inland waters, an estimation of both the water volumes and evolution of water temperature profiles is necessary. Water temperature observations of lakes, reservoirs, rivers, and wetlands are however sparse and spatially limited. So far, studies of energy fluxes and heat storage have been limited to individual lakes (Heiskanen et al., 2015; Strachan et al., 2016). To overcome this, global models are developed for estimating water temperatures on local, regional, and global scales.

In this study, we develop the first estimate of the global-scale heat uptake by inland waters over the period 1900–2020. To this end, we combine global lake and hydrological simulations from the Inter-Sectoral Model Intercomparison Project (ISIMIP) with a river temperature parameterization and spatially explicit data sets of lake abundance, reservoir area expansion, and lake depth. This enables us to quantify the heat uptake by natural lakes, reservoirs, and rivers. We do not consider the contribution of wetlands and floodplains, given their highly disperse spatial and temporal character and limited data availability. Next, we also quantify the redistribution of heat from ocean to land due to increased inland water storage as a result of the construction of reservoirs.

2. Data and Methods

2.1. Lake and Reservoir Heat Content

The ISIMIP initiative is a recent effort to provide consistent climate impact simulations across different sectors which allows for the integration and comparison of global hydrological and lake model simulations (Frieler et al., 2017). For lake water temperatures, we used the global ISIMIP2b simulations from three one-dimensional lake models: the Community Land Model 4.5 (Oleson et al., 2013) including the Lake, Ice, Snow, and Sediment Simulator (Subin et al., 2012), SIMSTRAT-UoG, a physically sophisticated k-ϵ model (Goudsmit et al., 2002) and the Arctic Lake Biogeochemistry Model (ALBM), a process-based lake biogeochemistry model (see supporting information Table S1; Tan et al., 2015). Following the ISIMIP2b protocol, simulations are performed at a 0.5° by 0.5° spatial resolution using bias-adjusted atmospheric forcing data from four Earth System Models (ESMs: GFDL-ESM2M, HadGEM2-ES, IPSL-CM5A-LR, and MIROC5). SIMSTRAT-UoG does not represent human influences, while Community Land Model 4.5 and ALBM assume that land use and human influences (irrigation extent, land use, population, and GDP) are constant at the 2005 level. We use ESM simulations for the historical period with historical climate and greenhouse gas conditions, ranging from 1900 to 2005 and Representative Concentration Pathway 6.0 simulations for the period 2006–2020 (Frieler et al., 2017). The lake models simulate a representative lake with a constant depth in each grid cell, of which the extent is given by the lake area fraction of that grid cell. The albedo and light attenuation coefficient are given by the models (Table S1, Potes et al., 2012). Using the four climate forcings for each lake model results in a total of 12 simulations of spatially explicit global-scale lake temperatures.

Global lake area distribution is given by the HydroLAKES dataset (Messager et al., 2016), containing 1.42 million individual polygons of natural lakes. This data set is linked to the Global Reservoir and Dam data set

v.1.3 (GRanD Lehner et al., 2011). We convert both HydroLAKES and GRanD polygons to lake area fraction on a 0.5° by 0.5° grid to match the ISIMIP resolution. Reservoir construction is provided by GRanD, and changes in reservoir area are accounted for by creating annual lake area fraction maps, in which reservoir areas are added in their year of construction. Natural lakes which become controlled by a dam are categorized as "natural lakes" based on information from GRanD. As GRanD provides construction years up to 2017, we assume a constant reservoir area from 2017 to 2020. Lake and reservoir depths are obtained from the Global Lake Database v.3 (GLDB, Choulga et al., 2014, 2019; Kourzeneva, 2010), providing estimates of mean lake depth for every land grid cell. These data are remapped from its original 30" (~1km grid) to the 0.5° by 0.5° resolution using bilinear interpolation.

Annual lake heat content Q_{lake} $[J]$, per grid cell is calculated as

$$Q_{lake} = c_{liq}\ A_{lake}\ \ \rho_{liq} \sum_{n=1}^{n=nlayers} T_n\ d_n$$

with c_{liq} $(Jkg^{-1}K^{-1})$ the specific heat capacity of liquid water (here taken constant at 4188 J $kg^{-1}K^{-1}$), A_{lake} (m^2) the lake area, ρ_{liq} (kg m^{-3}) the density of liquid water (here taken at 1000 kg m^{-3}), and the sum of annual mean temperatures T_n (K) over all lake layers, where d_n (m) is the layer thickness. As the layering of each lake model is different, lake heat per layer is rescaled by calculating the weights of the model layer depths relative to the models' grid cell lake depth. These weights are then applied on the grid cell lake depth from GLDB. This allows for a consistent volume computation. To also ensure a consistent lake coverage across the different lake models, the water temperatures are spatially interpolated to the lake coverage map derived from HydroLAKES using nearest neighbor remapping. The Caspian Sea is included in the analysis, as this inland sea is often not accounted for in ocean heat content estimates (e.g., Cheng et al., 2017). We define the spatial extent of natural lakes by the lake extent in 1900. Lake ice, with a heat capacity of 2117J kg^{-1} K^{-1}, is simulated by the lake models, but not included in the analysis due to constraints in model harmonisation. Inter-annual temperature changes of the liquid water below the ice cover is accounted for, but changes related to snow are not.

Heat content anomalies, hereafter denoted as heat uptake, are computed relative to the average lake heat content in 1900–1929, (hereafter referred to as pre-industrial period) and represent changes in lake and reservoir temperatures. Changes in the amount of water stored on land by the construction of reservoirs are also taken into account, thereby assuming the water temperature of the constructed reservoir is given by the grid cell lake temperature. We do not consider inter-annual variations in lake and reservoir volumes. Total annual global heat uptake is calculated by summing all grid cells.

As the lake models conserve energy, the heat related to freezing and melting of ice is included in the resulting water temperature given by the models. The relative contribution of this term in the total heat uptake can be determined separately by calculating Q_{phase} (J), the heat related to phase changes:

$$Q_{phase} = L_f\ \ \Delta d_{ice}\ \rho_{ice}\ A_{lake}$$

with L_f (Jkg^{-1}), the heat of fusion (3.337x10^5 Jkg^{-1}) and Δd_{ice} (m) the ice thickness.

2.2. River Heat Content

River water mass is retrieved from the grid-scale monthly river storage (kg m^{-2}) given by the two Global Hydrological Models from the ISIMIP 2b global water sector providing this variable: the Minimal Advanced Treatments of Surface Interaction and Runoff (Pokhrel et al., 2015) and WaterGAP2 (see Table S1 Müller Schmied et al., 2016), by multiplying with the grid cell area and taking the annual mean. Annual grid cell river water temperatures are estimated using the global nonlinear regression model of Punzet et al. (2012) with the global coefficients and an efficiency fit of 0.87. This regression prescribes river temperatures based on monthly gridded air temperatures, which are given by the four different ESM forcings (GFDL-ESM2M, HadGEM2-ES, IPSL-CM5A-LR, and MIROC5). River heat content, Q_{river} (J), is calculated as

$$Q_{river} = c_{liq}\ m_{river}\ T_{river}$$

with m_{river} (kg) the water storage in the grid cell rivers and T_{river} (K) the river temperature. As for lakes, river heat uptake is defined as the anomaly compared to the average river heat content in the reference period 1900–1929 and consists of the change in temperature and the change in water stored in the rivers. This approach uses a total of eight ISIMIP simulations. The set-up of the models, dictated by the ISIMIP protocol, allows the direct comparison of the resulting lake, reservoir, and river heat uptake.

Table 1
Total Heat Uptake and Trend for the Different Inland Water Components

	Heat uptake	Heat flux (1991–2020)	Trend (1991–2020)
Natural lakes	$2.87 \pm 2.01 \times 10^{20}$J	0.1 ± 0.04 W m^{-1}	10.2×10^{18} J yr^{-1}
Reservoirs	$0.06 \pm 0.03 \times 10^{20}$J	0.02 ± 0.001W m^{-1}	0.2×10^{18}J yr^{-1}
Rivers	$-0.36 \pm 1.20 \times 10^{20}$J	0.05 ± 0.05W m^{-1}	2.7×10^{18}J yr^{-1}
Total heat uptake	$2.57 \pm 3.23 \times 10^{20}$J	0.09 ± 0.04W m^{-1}	13.1×10^{18}J yr^{-1}
Redistribution by reservoir expansion	$26.76 \pm 2.13 \times 10^{20}$J	0.52 ± 0.30W m^{-1}	15.2×10^{18}J yr^{-1}

Note. Heat uptake is calculated as the average heat content of 2011–2020 relative to the reference period 1900–1929. Uncertainties are given by the ensemble standard deviation of the used simulations. Heat fluxes are calculated as the difference in heat uptake between 2020 and 1991, divided by the area (lake and reservoir area from HydroLAKES, and the river surface area from Allen & Pavelsky, 2018). Trends in heat content in 1991–2020 are calculated using a linear regression.

3. Inland Water Heat Uptake

Natural lakes have taken up $2.9 \pm 2.0 \times 10^{20}$ J ($\pm$ one standard deviation of the 12 simulations) averaged over the period 2011–2020, relative to preindustrial times (1900–1929; Table 1), due to an increase of lake water temperatures integrated over the lake column. The dip in heat uptake in 1960–1978 originates from a decrease in surface temperature in the GCM forcings associated with global dimming (Frieler et al., 2017; Wild, 2009). From the 1980s onwards, lake heat uptake increased continuously, following the trend of increasing atmospheric temperatures (Figures 1a, supporting information Figure S2). In the last 30 years, the mean trend in global lake heat uptake of the model simulations is 10.2×10^{18} J year^{-1}. The heat uptake related to melting of the ice in 1900–2020 is negligible, as it contributes only 0.004% ($8.8 \pm 10.4 \times 10^{15}$ J) to the total heat uptake by natural lakes.

The construction of dams and the resulting artificial reservoirs have increased global lake volume by 3.2% (supporting information Figure S1b, Messager et al., 2016). The steep increase in reservoir heat uptake from the 1980s onwards stems from the combination of accelerated reservoir construction, making more water on land available for warming, and regional emergence of warming signals due to climate change during this period (Figure 1b). In total, reservoirs have taken up $5.9 \pm 2.7 \times 10^{18}$ J on average in the period 2011–2020, compared to pre-industrial times (Table 1).

Global heat uptake by rivers encompasses large uncertainties and no detectable trend. In the late 1960s the ensemble mean heat uptake shifts to overall negative heat uptake compared to pre-industrial values (Figure 1c). Global-scale stream temperatures show a clear positive trend, reflecting the increase in air temperatures (supporting information, Figure S3a–d). However, global-scale river storage is marked by large inter-annual variability for both global hydrological models (Figure S3e–l), thereby effectively masking the positive temperature trend in the resulting river heat uptake. River storage evolution is dictated mainly by the ESM forcing, as differences in river storage between the four different ESM forcings are more pronounced than between the two global hydrological models (Figure S3). Altogether, with a heat uptake of $-0.36 \pm 3.2 \times 10^{20}$ J averaged for 2011 to 2020, compared to pre-industrial times, rivers contribute negatively to the total heat uptake by inland waters, but their contribution is accompanied by a large variability, as well as uncertainty originating from the spread across climate forcings.

The total heat uptake in inland waters is thus dominated by the heat uptake of natural lakes, accounting for 111.7% of the average total net increase by 2020, while reservoir heating has taken up 2.3% and rivers contributed negatively with -14% in 2020, but the latter with a large uncertainty (Figure 3a).

Most lake heat uptake is concentrated in the major lake regions of the world. The Laurentian Great Lakes, including Lakes Superior, Michigan, Huron, Erie, and Ontario in central North America make up 12.4% of global lake volume (Messager et al., 2016). These lakes all demonstrate a steady increase in heat uptake from the 1980s onwards (Figure 2b), resulting in a total uptake of $2.28 \pm 1.64 \times 10^{19}$ J (8.9% of global inland water heat uptake) compared to pre-industrial times, with a trend of 6.8×10^{17} J year^{-1} over the last 30 years. The spatial pattern of heat uptake is mainly dictated by the bathymetry and resulting lake volume: the deeper Lake Michigan and Lake Superior have taken up more heat compared to the other lakes, while the much shallower Lake Erie has the lowest heat uptake estimates (Figure 2a).

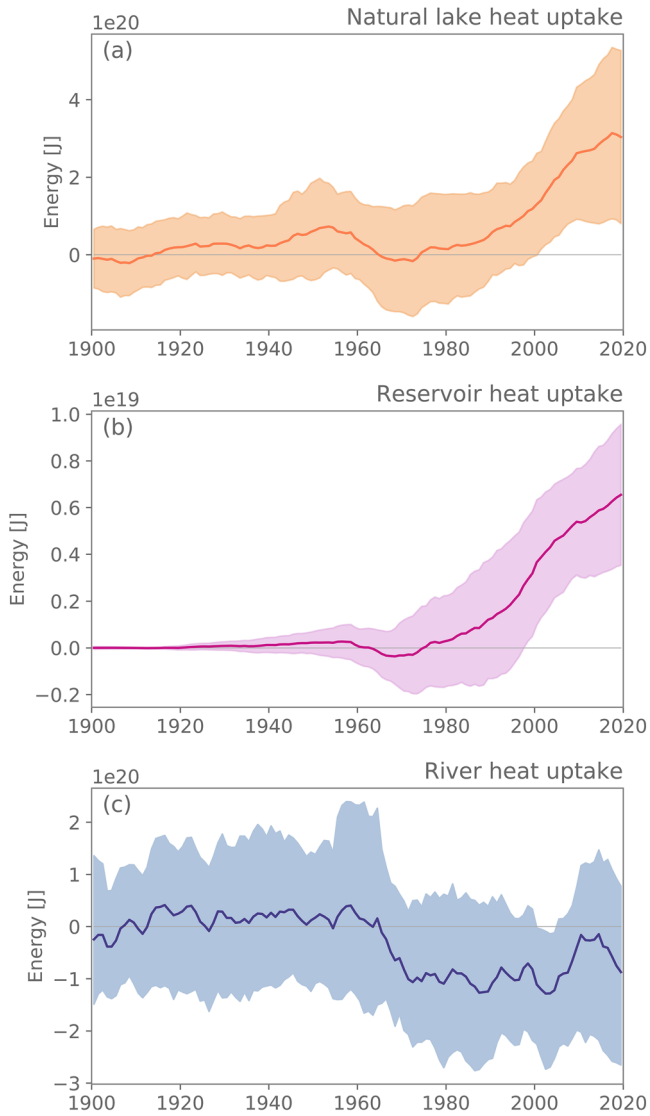

Figure 1. Heat uptake by natural lakes (a), reservoirs (b), and rivers (c). Shown are 10-year moving means relative to the 1900–1929 reference period. Note the different y-axis scales. Color shades represent uncertainty range shown as the standard deviation of the used simulations.

The African Great Lakes region in East Africa, consisting of Lake Victoria, Tanganyika, Kivu, Kyoga, Albert, and Edward (12.38% of global lake volume, Messager et al., 2016), is known to affect the local weather and climate conditions (Thiery et al., 2014, 2015, 2016, 2017; Vanderkelen et al., 2018b; Van de Walle et al., 2019), and their water temperatures are observed to be warming (Tierney et al., 2010). We find that the heat uptake is largest in Tanganyika, the lake with the highest volume in the region (Figure 2c). Overall, the African Great Lakes show an increase in heat over the whole study period (Figure 2d, a total heat uptake of $4.04 \pm 1.62 \times 10^{19}$ J, 15.7% of global inland water heat uptake). The Great European lakes, including Lake Ladoga and Onega show a smaller increase compared to other major lake regions, corresponding to the smaller volume of the lakes, but the lake heat content shows a sudden increase from the 1990s (Figures 2e and 2f; total heat uptake of $2.31 \pm 1.13 \times 10^{18}$ J, 0.9% of global inland water heat uptake). The Amazon, world's highest discharge river, depicts no temporal trend in river heat uptake, but the uncertainty is large, mainly owing to the diverging river mass estimations (Figure 2h; heat uptake of $0.18 \pm 1.50 \times 10^{20}$ J, 7% of global inland water heat uptake). Heat uptake increases towards the river mouth, as the water volume increases (Figure 2g). To summarize, the global picture of heat uptake is confirmed at the regional scale by all model combinations.

10.1029/2020GL087867

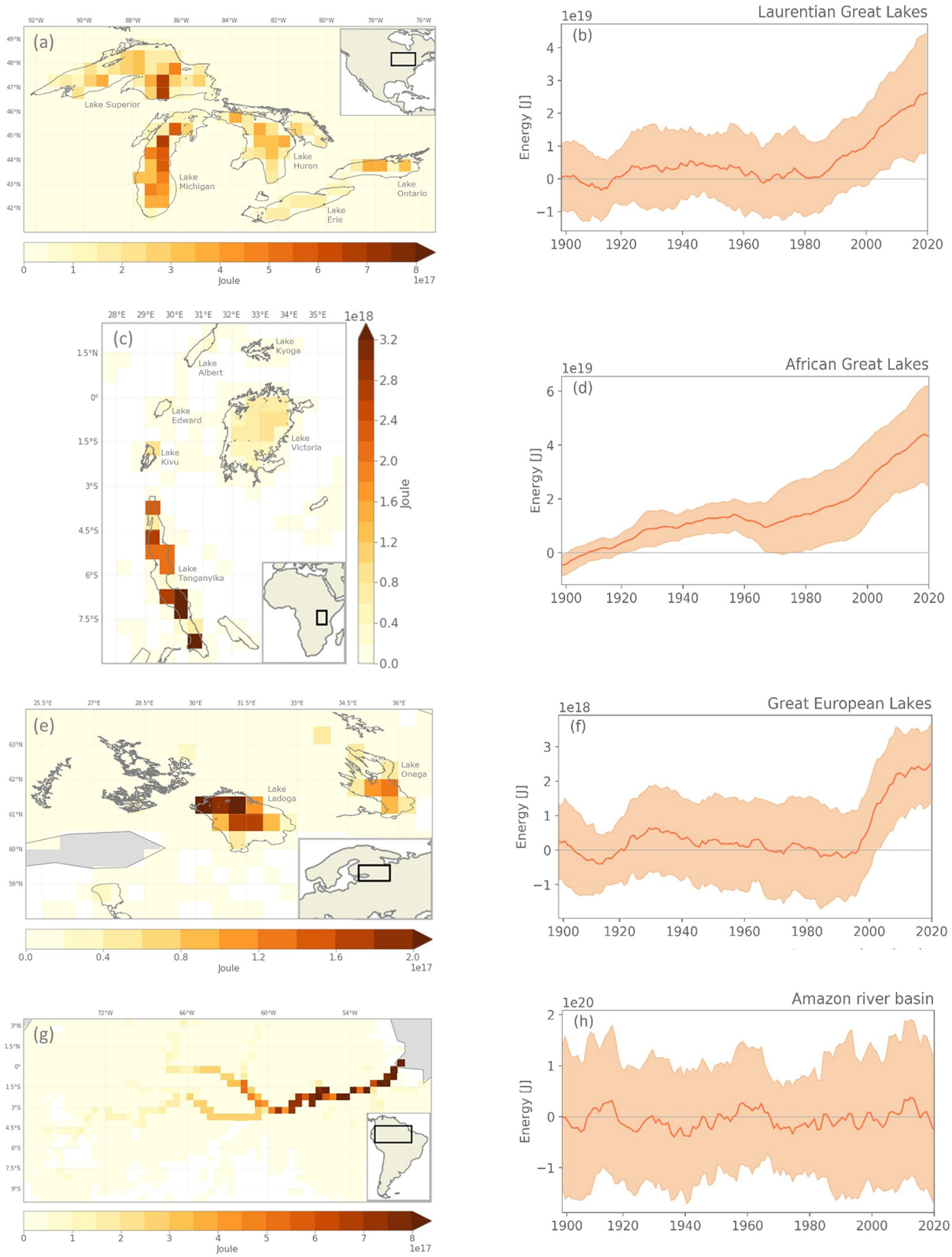

Figure 2. Heat uptake by the Laurentian Great lakes (a–b), the African Great Lakes (c–d), the Great European Lakes (e–f), and the Amazon River (g–h). The maps represent the average heat uptake during the 2001–2020 period with the grey colors indicating ocean grid cells, and white colors grid cells without water. The graphs show 10-year moving means, where the color shades represent uncertainty range shown as the standard deviation of the used simulations. The reference period is 1900–1929. Note the different y-axis scales.

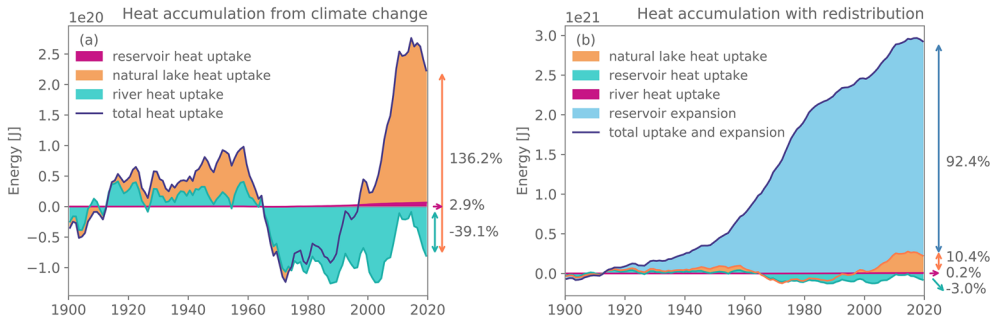

Figure 3. Inland water heat accumulation from climate change (a) and including redistribution by reservoir construction (b). Shown are 10-year moving ensemble means relative to the 1900–1929 reference period. Note the different y-axis scales.

4. Heat Redistribution Due to Reservoir Area Expansion

In the second half of the 20th century, reservoir capacity strongly increased, raising the water volume stored on land and offsetting sea level rise by 30 mm (supporting information Figure S1b, Chao et al., 2008; Lehner et al., 2011; Pokhrel et al., 2012). This extra water stored on land does not only increase the potential of the land surface for taking up excess atmospheric heat (Section 3), but also carries energy in itself. By constructing reservoirs, humans are thus not only redistributing mass from the oceans to the land, but also the thermal energy carried within this water. This heat redistribution by reservoir expansion is growing over time, following the increasing number of reservoirs constructed (Figure 3b). During the historical period, $26.8 \pm 2.1 \times 10^{20}$ J of heat was redistributed from ocean to land, exceeding inland water heat uptake from climate change by a factor of ~10.4.

5. Discussion and Conclusions

Large lakes take up most heat, as they have the largest volume to warm up. The increase in lake heat content complies with recent observations of increasing lake surface temperatures and reported changes in mixing regimes (O'Reilly et al., 2015; Woolway & Merchant, 2019) and is robust for different lake regions. The difference between the three lake models (Figure S2) could arise from differences in the structure of the models, like lake layers and internal physics.

River heat uptake is negative in most simulations during the second half of the 20th century. This seemingly contradictory result stems from a decrease in river storage, which could be attributed to less precipitation or the construction of reservoirs, lowering water flow in rivers or to drying of rivers by increased land evaporation due to global warming or increased water use. These changes in river storage should, however, be taken with care, as the uncertainties are very large. In addition, no conclusions can be made about global trends in observed streamflow, because changes in streamflow and the hydrological conditions causing it, are characterized by complex spatial patterns (Gudmundsson et al., 2019; Müller Schmied et al., 2016).

The quantification of heat uptake facilitates comparison of the effects of climate change on different components of the climate system. Globally, inland waters have taken up ~0.08% of heat compared to oceans. The continental heat uptake occurs through a heat flux into the solid surface of the lithosphere and has been estimated between 9.1 and 10.4×10^{21} J (Beltrami et al., 2002; Huang, 2006) for the period 1950–2000 based on borehole temperature observations. Estimates based on the Coupled Model Intercomparison Project Phase 5 (CMIP5) are consistently lower ($1 \pm 5 \times 10^{21}$ J), mainly due to the limited depth of the bottom boundary of the land surface schemes of the Earth system models (Cuesta-Valero et al., 2016). Relative to the geophysical estimate reported by Beltrami et al. (2002), the share of inland waters is ~3.6%, while inland waters cover about ~2.58% of the global continental area. This comparison has to be taken with care, as the borehole-based estimations of heat uptake are only quantified until 2000 and surface air temperatures have risen at record rates since then (Rhein et al., 2013).

The redistribution of heat by reservoir construction is equivalent to ~38% of the land mass heat uptake. This is mainly a transfer of water mass with its associated internal energy. As it only increases the potential of storing extra heat on land, the redistribution has little influence on the potential heat uptake on a global scale. In particular, the warming of the water in the created reservoirs might cause local impacts such as masking

surface temperature increase on diurnal and seasonal timescales by their buffering capacity. In addition, the extra continental water storage by reservoir expansion could have a dampening effect on local temperature extremes and could affect river temperatures downstream. It is therefore important to account for reservoir expansion and resulting heat redistribution in Earth System Models, to increase our understanding of how reservoirs affect the climate (Pokhrel et al., 2016; Wada et al., 2017). Capturing heat redistribution by reservoir expansion could also increase the quality of climate change projections on regional to global scales.

There are several opportunities to refine the heat uptake calculations presented in this study. First, the volume calculation does not account for lake hypsometry. By using average lake depths to multiply with lake area, the resulting total lake volumes are reasonable, as most lakes have a linear hypsometric relationship (Busker et al., 2019). This rectangular hypsometry assumption results in relatively higher weights for the deeper lake layers, which makes our heat uptake estimates more conservative. Second, apart from reservoir construction, the heat calculation does not account for variations in lake and reservoir volumes, while changes in river storage are included. This could have important effects, especially for lakes with a high inter-annual variability. Third, variations in heat capacity are not considered in our analysis, which could lead to a lower estimate of heat uptake as the specific capacity of ice is lower than that of water (2117 J kg^{-1} K^{-1} compared to 4188 J kg^{-1} K^{-1}, respectively). Next, variations in salinity of inland waters are not included. Evaluating the modeled lake heat uptake with observations from individual lakes reveals substantial inconsistencies (see supporting information), which are partly due the result of model uncertainty, but also highlight the need for constraining parameter values such as water transparency, refining the ISIMIP simulation setup to include observed atmospheric forcing and increasing the collection of long-term lake temperature profiles. Furthermore, by using global lake and hydrological models driven by ESM forcings, an extra uncertainty related to climate sensitivity is added to the calculations. Despite these limitations, this study is the first step towards estimating heat uptake by inland waters.

In this study, we show that inland water heat uptake during the historical period is small compared to continental heat uptake, but in line with the surface area of inland waters relative to land. Furthermore, we highlight that by constructing reservoirs, humans have redistributed heat from the ocean to land as well as increased the potential of storing more heat on land, given the higher heat capacity of water compared to land. Compared to the other components of the Earth system, this is a small term, but locally the impacts might be large. By providing a first estimate of inland water heat uptake, this study provides new advances in the quantification of the global heat budget.

Acknowledgments
All ISIMIP2b simulations used are publicly available through the Earth System Grid Federation (ESGF, https://esgf-data.dkrz.de/). The HydroLAKES dataset is available at https://www.hydrosheds.org/page/hydrolakes, GRanD at https://globaldamwatch.org/, GLDB at https://www.lakemodel.net/ and observations from the North Temperate Lakes LTER at https://lter.limnology.wisc.edu/about/lakes. Scripts used are available at: https://github.com/VUB-HYDR/2020_Vanderkelen_etal_GRL. Inne Vanderkelen is a research fellow at the Research Foundation Flanders (FWOTM920). Wim Thiery acknowledges the Uniscientia Foundation and the ETH Zurich Foundation for their support. Zeli Tan is supported by the U.S. DOEs Earth System Modeling program through the Energy Exascale Earth System Model (E3SM) project. We are grateful to the Potsdam Institute for Climate Impact Research (PIK) for initiating and coordinating the ISIMIP initiative and to the modeling centers for making their simulations available through ESGF. Computational resources and services were provided by the Shared ICT Services Centre funded by the Vrije Universiteit Brussel, the Flemish Supercomputer Center (VSC) and FWO.

References

Adrian, R., O'reilly, C. M., Zagarese, H., Baines, S. B., Hessen, D. O., Keller, W., et al. (2009). Lakes as sentinels of climate change. *Limnology and Oceanography*, *54*(6), 2283–2297.

Allen, G. H., & Pavelsky, T. (2018). Global extent of rivers and streams. *Science*, *361*(6402), 585–588. https://doi.org/10.1126/science.aat063

Beltrami, H., Smerdon, J. E., Pollack, H. N., & Huang, S. (2002). Continental heat gain in the global climate system. *Geophysical Research Letters*, *29*(8), 1167. https://doi.org/10.1029/2001GL014310

Bindoff, N. L., Cheung, W. W. L., Kairo, J. G., Arístegui, J., Guinder, V. A., Hallberg, R., et al. (2019). Changing Ocean, Marine Ecosystems, and Dependent Communities. In *Ipcc special report on the ocean and crosphere in a changing climate*.

Busker, T., De Roo, A., Gelati, E., Schwatke, C., Adamovic, M., Bisselink, B., et al. (2019). A global lake and reservoir volume analysis using a surface water dataset and satellite altimetry. *Hydrology and Earth System Sciences*, *23*(2), 669–690. https://doi.org/10.5194/hess-23-669-2019

Chao, B. F., Wu, Y. H., & Li, Y. S. (2008). Impact of artificial reservoir water impoundment on global sea level. *Science*, *320*(5873), 212–214. https://doi.org/10.1126/science.1154580

Cheng, L., Trenberth, K. E., Fasullo, J., Boyer, T., Abraham, J., & Zhu, J. (2017). Improved estimates of ocean heat content from 1960 to 2015. *Science Advances*, *3*(3), 1–10. https://doi.org/10.1126/sciadv.1601545

Choulga, M., Kourzeneva, E., Balsamo, G., Boussetta, S., & Wedi, N. (2019). Upgraded global mapping information for earth system modelling: An application to surface water depth at the ECMWF. *Hydrology and Earth System Sciences*, *23*(10), 4051–4076. https://doi.org/10.5194/hess-23-4051-2019

Choulga, M., Kourzeneva, E., Zakharova, E., & Doganovsky, A. (2014). Estimation of the mean depth of boreal lakes for use in numerical weather prediction and climate modelling. *Tellus, Series A: Dynamic Meteorology and Oceanography*, *66*(1), 21295. https://doi.org/10.3402/tellusa.v66.21295

Cuesta-Valero, F. J., García-García, A., Beltrami, H., & Smerdon, J. E. (2016). First assessment of continental energy storage in CMIP5 simulations. *Geophysical Research Letters*, *43*, 5326–5335. https://doi.org/10.1002/2016GL068496

Frieler, K., Lange, S., Piontek, F., Reyer, C. P. O., Schewe, J., Warszawski, L., et al. (2017). Assessing the impacts of 1.5 C global warming - simulation protocol of the Inter-Sectoral Impact Model Intercomparison Project (ISIMIP2b). *Geoscientific Model Development*, *10*(12), 4321–4345. https://doi.org/10.5194/gmd-10-4321-2017

Goudsmit, G. H., Burchard, H., Peeters, F., & Wüest, A. (2002). Application of k-ϵ turbulence models to enclosed basins: The role of internal seiches. *Journal of Geophysical Research*, *107*(12), 3230. https://doi.org/10.1029/2001JC000954

Gudmundsson, L., Leonard, M., Do, H. X., Westra, S., & Seneviratne, S. I. (2019). Observed trends in global indicators of mean and extreme streamflow. *Geophysical Research Letters*, *46*, 756–766. https://doi.org/10.1029/2018GL079725

Heiskanen, J. J., Mammarella, I., Ojala, A., Stepanenko, V., Erkkilä, K. M., Miettinen, H., et al. (2015). Effects of water clarity on lake stratification and lake-atmosphere heat exchange. *Journal of Geophysical Research: Atmospheres*, *120*, 7412–7428. https://doi.org/10.1002/2014JD022938

Huang, S. (2006). 1851-2004 annual heat budget of the continental landmasses. *Geophysical Research Letters*, *33*, L04707. https://doi.org/10.1029/2005GL025300

Kourzeneva, E. (2010). External data for lake parameterization in numerical weather prediction and climate modeling. *Boreal Environment Research*, *15*(2), 165–177. https://doi.org/10.3402/tellusa.v64i0.15640

Lehner, B., Liermann, C. R., Revenga, C., Vörömsmarty, C., Fekete, B., Crouzet, P., et al. (2011). High-resolution mapping of the world's reservoirs and dams for sustainable river-flow management. *Frontiers in Ecology and the Environment*, *9*(9), 494–502. https://doi.org/10.1890/100125

Messager, M. L., Lehner, B., Grill, G., Nedeva, I., & Schmitt, O. (2016). Estimating the volume and age of water stored in global lakes using a geo-statistical approach. *Nature Communications*, *7*, 13603. https://doi.org/10.1038/ncomms13603

Müller Schmied, H., Adam, L., Eisner, S., Fink, G., Florke, M., Kim, H., et al. (2016). Variations of global and continental water balance components as impacted by climate forcing uncertainty and human water use. *Hydrology and Earth System Sciences*, *20*(7), 2877–2898. https://doi.org/10.5194/hess-20-2877-2016

O'Reilly, C. M., Sharma, S., Gray, D. K., Hampton, S. E., Read, J. S., Rowley, R. J., et al. (2015). Rapid and highly variable warming of lake surface waters around the globe. *Geophysical Research Letters*, *42*, 10,773–10,781. https://doi.org/10.1002/2015GL066235

Oleson, K. W., Lead, D. M. L., Bonan, G. B., Drewniak, B., Huang, M., Koven, C. D., et al. (2013). Technical description of version 4.5 of the ommunity Land Model (CLM) coordinating lead authors: NCAR/TN-503+STR. https://doi.org/10.5065/D6RR1W7M

Pekel, J. F., Cottam, A., Gorelick, N., & Belward, A. S. (2016). High-resolution mapping of global surface water and its long-term changes. *Nature*, *540*(7633), 418–422. https://doi.org/10.1038/nature20584

Pokhrel, Y. N., Hanasaki, N., Wada, Y., & Kim, H. (2016). Recent progresses in incorporating human land-water management into global land surface models toward their integration into Earth system models. *Wiley Interdisciplinary Reviews: Water*, *3*(4), 548–574. https://doi.org/10.1002/wat2.1150

Pokhrel, Y. N., Hanasaki, N., Yeh, P. J.-F., Yamada, T. J., Kanae, S., & Oki, T. (2012). Model estimates of sea-level change due to anthropogenic impacts on terrestrial water storage. *Nature Geoscience*, *5*(6), 389–392. https://doi.org/10.1038/ngeo1476

Pokhrel, Y. N., Koirala, S., Yeh, P. J.-F., Hanasaki, N., Longuevvergne, L., Kanae, S., & Oki, T. (2015). Incorporation of groundwater pumping in a global Land Surface Model with the representation of human impacts. *Water Resources Research*, *51*, 78–96. https://doi.org/10.1002/2014WR015602

Potes, M., Costa, M. J., & Salgado, R. (2012). Satellite remote sensing of water turbidity in Alqueva reservoir and implications on lake modelling. *Hydrology and Earth System Sciences*, *16*(6), 1623–1633. https://doi.org/10.5194/hess-16-1623-2012

Punzet, M., Voß, F., Voß, A., Kynast, E., & Bärlund, I. (2012). A global approach to assess the potential impact of climate change on stream water temperatures and related in-stream first-order decay rates. *Journal of Hydrometeorology*, *13*(3), 1052–1065. https://doi.org/10.1175/JHM-D-11-0138.1

Rhein, M., Rintoul, S. R., Aoki, S., Campos, E., Chambers, D., Feely, R. A., et al. (2013). Observations: Ocean. In T. F. Stocker, D. Qin, G.-K. Plattner, et al. (Eds.), *Climate change 2013—The physical science basis. contribution of working group i to the fifth assessment report of the intergovernmental panel on climate change* (pp. 465–570). Cambridge, United Kingdom and New York, NY, USA: Cambridge University Press. https://doi.org/10.1017/CBO9781107415324.015

Schewe, J., Heinke, J., Gerten, D., Haddeland, I., Arnell, N. W., Clark, D. B., et al. (2014). Multimodel assessment of water scarcity under climate change. *Proceedings of the National Academy of Sciences of the United States of America*, *111*(9), 3245–3250.

Schneider, P., & Hook, S. J. (2010). Space observations of inland water bodies show rapid surface warming since 1985. *Geophysical Research Letters*, *37*, L22405. https://doi.org/10.1029/2010GL045059

Strachan, I. B., Tremblay, A., Pelletier, L., Tardif, S., Turpin, C., & Nugent, K. A. (2016). Does the creation of a boreal hydroelectric reservoir result in a net change in evaporation? *Journal of Hydrology*, *540*, 886–899. https://doi.org/10.1016/j.jhydrol.2016.06.067

Subin, Z. M., Riley, W. J., & Mironov, D. (2012). An improved lake model for climate simulations: Model structure, evaluation, and sensitivity analyses in CESM1. *Journal of Advances in Modeling Earth Systems*, *4*, M02001. https://doi.org/10.1029/2011MS000072

Tan, Z., Zhuang, Q., & Anthony, K. W. (2015). Modeling methane emissions from arctic lakes: Model development and site-level study. *Journal of Advances in Modeling Earth Systems*, *7*, 459–483. https://doi.org/10.1002/2014MS000344

Thiery, W., Davin, E. L., Lawrence, D. M., Hirsch, A. L., Hauser, M., & Seneviratne, S. I. (2017). Present-day irrigation mitigates heat extremes. *Journal of Geophysical Research: Atmospheres*, *122*, 1403–1422. https://doi.org/10.1002/2016JD025740

Thiery, W., Davin, E. L., Panitz, H.-J., Demuzere, M., Lhermitte, S., & van Lipzig, N. (2015). The impact of the African Great Lakes on the regional climate. *Journal of Climate*, *28*(10), 4061–4085. https://doi.org/10.1175/JCLI-D-14-00565.1

Thiery, W., Davin, E. L., Seneviratne, S. I., Bedka, K., Lhermitte, S., & Van Lipzig, N. P. M. (2016). Hazardous thunderstorm intensification over Lake Victoria. *Nature Communications*, *7*, 12786. https://doi.org/10.1038/ncomms12786

Thiery, W., Stepanenko, V. M., Fang, X., Jöhnk, K. D., Zhongshun, L., Martynov, A., et al. (2014). LakeMIP Kivu: evaluating the representation of a large, deep tropical lake by a set of one-dimensional lake models. *Tellus A*, *66*, 21390. https://doi.org/10.3402/tellusa.v66.21390

Tierney, J. E., Russell, J. M., & Huang, Y. (2010). A molecular perspective on Late Quaternary climate and vegetation change in the Lake Tanganyika basin, East Africa. *Quaternary Science Reviews*, *29*(5-6), 787–800. https://doi.org/10.1016/j.quascirev.2009.11.030

Trenberth, K. E. (2009). An imperative for climate change planning: tracking Earth's global energy. *Current Opinion in Environmental Sustainability*, *1*(1), 19–27. https://doi.org/10.1016/j.cosust.2009.06.001

Van de Walle, J., Thiery, W., Brousse, O., Souverijns, N., Demuzere, M., & van Lipzig, N. P. M. (2019). A convection-permitting model for the Lake Victoria Basin: Evaluation and insight into the mesoscale versus synoptic atmospheric dynamics. *Climate Dynamics*, *1*, 3. https://doi.org/10.1007/s00382-019-05088-2

Vanderkelen, I., van Lipzig, N. P. M., & Thiery, W. (2018a). Modelling the water balance of Lake Victoria (East Africa)-Part 1: Observational analysis. *Hydrology and Earth System Sciences*, *22*(10), 5509–5525. https://doi.org/10.5194/hess-22-5509-2018

Vanderkelen, I., van Lipzig, N. P. M., & Thiery, W. (2018b). Modelling the water balance of Lake Victoria (East Africa) - Part 2: Future projections. *Hydrology and Earth System Sciences*, *22*(10), 5527–5549. https://doi.org/10.5194/hess-22-5527-2018

Wada, Y., Bierkens, M. F. P., De Roo, A., Dirmeyer, P. A., Famiglietti, J. S., Hanasaki, N., et al. (2017). Human water interface in hydrological modelling: Current status and future directions. *Hydrology and Earth System Sciences*, *21*, 4169–4193. https://doi.org/10.5194/hess-21-4169-2017

Wild, M. (2009). Global dimming and brightening: A review. *Journal of Geophysical Research*, *114*, D00D16. https://doi.org/10.1029/2008JD011470

Woolway, R. I., & Merchant, C. J. (2019). Worldwide alteration of lake mixing regimes in response to climate change. *Nature Geoscience*, *12*(4), 271–276. https://doi.org/10.1038/s41561-019-0322-x